Reprinted from

APPLIED PHYSICS EXPRESS

Power Optimization of a Planar Single-Channel Shim Coil for a Permanent Magnet Circuit

Yasuhiko Terada, Keiichiro Ishi, Daiki Tamada, and Katsumi Kose

Appl. Phys. Express **6** (2013) 026701

Applied Physics Express 6 (2013) 026701
http://dx.doi.org/10.7567/APEX.6.026701

Power Optimization of a Planar Single-Channel Shim Coil for a Permanent Magnet Circuit

Yasuhiko Terada*, Keiichiro Ishi, Daiki Tamada, and Katsumi Kose

Institute of Applied Physics, University of Tsukuba, Tsukuba, Ibaraki 305-8573, Japan
E-mail: terada@bk.tsukuba.ac.jp

Received December 7, 2012; accepted December 26, 2012; published online January 22, 2013

We propose a new method of designing a power-optimized single-channel shim coil (SCSC), which enables high homogeneity in the magnetic field of a magnetic resonance imaging system. The design method is based on a superposition of multiple circular currents to account for the power dissipated in the current-carrying coils. With a power-optimized SCSC, magnetic field inhomogeneity is largely corrected and there is negligible degradation of the magnetic field in continuous use. © 2013 The Japan Society of Applied Physics

Homogeneity in the magnetic field (B_0) is critical to achieving high image quality in magnetic resonance imaging (MRI). B_0 inhomogeneity in an MRI magnet is often corrected by multiple shim coils with adjustable currents, each of which is designed to correct a specific spherical-harmonic distribution in the B_0 inhomogeneity (such as $2Z^2$–X^2–Y^2, X^2–Y^2, X^2–Z^2, Y^2–Z^2, XY, YZ, or ZX).[1,2] In contrast to these multiple shim coils, a single-channel shim coil (SCSC)[3–6] uses a single coil with an adjustable current, whose pattern is designed by calculating a superposition of multiple shim-coil currents. SCSCs are particularly suited to permanent magnet circuits, because the spacing of the magnet gap or bore can be reduced and the power supply system can be simplified. Recently, it has been shown that the use of SCSCs can enable compensation for local high-order spatial inhomogeneity that cannot be corrected by magnet shimming.[5,6]

In a permanent magnetic circuit, the B_0 spatial variation and homogeneity are sensitive to thermal changes of the pole pieces.[7] In most cases, moreover, an SCSC is installed near the pole pieces, and the heat generated by the SCSC will cause undesired changes in the magnetic properties of the pole pieces. Therefore, continuous use of the SCSC often degrades B_0 homogeneity, particularly when a large current is required for shimming. The degradation in B_0 homogeneity can result in severe deterioration in image qualities (such as signal loss, image distortion, or image blurring). Despite its importance, the power dissipated by an SCSC has yet to be considered in its design.

In this study, we propose a new method of designing an SCSC, which is based on a power optimization approach. We then show that the use of a power-optimized SCSC leads to less heat generation and suppresses the degradation of B_0 homogeneity to a negligible level.

The MRI system considered in our shim design comprised a C-shaped Nd–Fe–B permanent magnet (Shin-Etsu Chemical), a gradient coil set, a radiofrequency probe, and an MRI console. The specifications for the magnet included a field strength of 0.3 T, a homogeneity of 24.8 ppm over a $12 \times 16 \times 5\,\mathrm{cm}^3$ diameter ellipsoidal volume (DEV), a gap width of 12 cm, dimensions of $40 \times 57 \times 41\,\mathrm{cm}^3$, and a weight of 450 kg. $B_0(\mathbf{r})$ in the central ellipsoidal area ($12 \times 16 \times 5\,\mathrm{cm}^3$ DEV) was measured by a conventional MRI-based phase-shift method [a spin echo sequence with field of view (FOV) $= 22 \times 22 \times 6\,\mathrm{cm}^3$, matrix $= 256 \times 64 \times 32$, repetition time (TR) $= 160$ ms, echo time (TE) $= 16$ ms, and phase-shift time $= 300\,\mu$s]. The MRI phantom used was a phantom made of a cylindrical acrylic container (diameter : 200 mm, height : 55 mm) filled with $CuSO_4$-doped water.

The method of designing the SCSC was based on the superposition of multiple circular currents (MCCs),[5,8,9] which account for the power dissipation. In the MCC method, the magnetic field B_s generated by the SCSC is a linear combination of the magnetic fields B_{ij} generated by circular unitary currents placed on an $n \times m$ elliptical grid, such that $B_s = \sum_{i,j} c_{ij} B_{ij}(\mathbf{r})$. Here, c_{ij} is the coefficient used in the linear combination for the circular current flowing at position (i, j). The field inhomogeneity $\Delta B_0(\mathbf{r})$ was calculated as $\Delta B_0(\mathbf{r}) = B_0(\mathbf{r}) - B_S(\mathbf{r})$, where $B_0(\mathbf{r})$ is the magnetic field measured at a position $\mathbf{r}$ with respect to the center of the magnet gap. To evaluate the B_0 inhomogeneity and power dissipated by the coil, an optimization function

$$f = \Delta B_{\mathrm{rms}} + \lambda \sum_{i,j} c_{ij}^2,$$

was introduced, where ΔB_{rms} is the root mean square (RMS) of ΔB_0 and λ denotes a weighting factor for power dissipation. The coefficients c_{ij} were optimized to minimize f for a given λ using a quasi-Newton method. When $\lambda = 0$, the optimization problem corresponds to a previously reported method that excluded power dissipation effects.[5]

The coil winding patterns were then derived using a stream function (SF) method, from the current density for the SCSC, $\mathbf{J}_s = \sum_{i,j} c_{ij} G(\sigma) * \mathbf{J}_{ij}$, where $\mathbf{J}_{ij}$ is the current density of each coil element, $G(\sigma)$ is a normalized Gaussian filter with standard deviation σ, and $*$ denotes the convolution operation.[4,5]

For the MCC method, the number, diameter, and interval of circular currents were set to be 8×10, 15 mm, and 17 mm, respectively. For the SF method, the number of contour lines was 40. Because the value of σ affects the coil performance (namely, attainable B_0 homogeneity and power dissipation), we first investigated the dependences of RMS ΔB_0 and power dissipation P on σ for $\lambda = 0$ [Fig. 1(a)]. The power dissipation could be reduced by increasing σ, while the inhomogeneity increased with σ. This can be explained as follows. When a larger value of σ is chosen in the SF method, $\mathbf{J}_s$ becomes smoother because of stronger Gaussian filtering and a sparser coil pattern is obtained, which leads to lower power dissipation. Meanwhile, a larger σ also leads to a reduction in the attainable B_0 homogeneity because of a larger error between $\mathbf{J}_s$ and $\mathbf{J}_{ij}$. The same tendency was seen in the calculation for other values of λ. Accordingly, we determined that $\sigma = 58.2$ mm was the critical value, above which RMS ΔB_0 increased with σ.

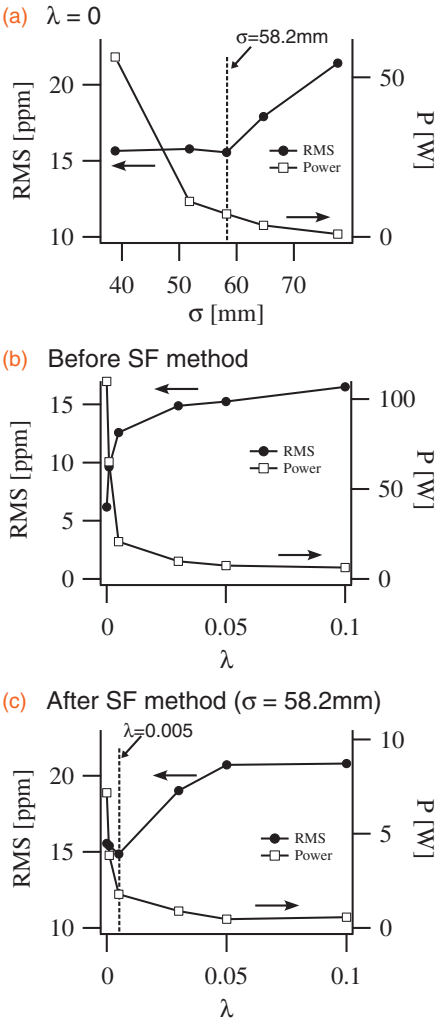

Fig. 1. Dependence of RMS ΔB_0 and power dissipation P on the design parameters. (a) Dependence on σ for $\lambda = 0$, where power dissipation is not considered. (b) and (c) Dependence on λ (b) before and (c) after the SF method was applied. $\sigma = 58.2$ mm in (c).

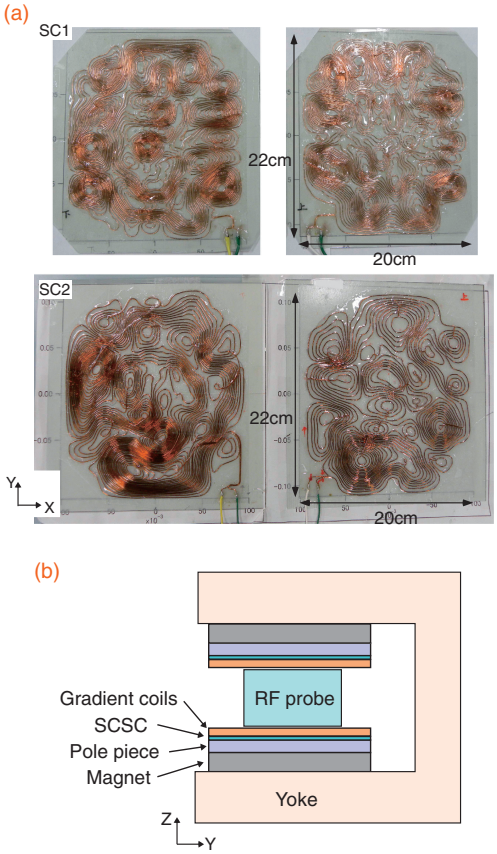

Fig. 2. (a) Fabricated SCSCs (nonoptimized SC1 and power-optimized SC2). (b) Schematic of the magnetic circuit, gradient coils, SCSC, and radiofrequency probe. The magnet circuit comprised of the pole piece, magnet, and yoke.

Several SCSCs were then designed with various values for λ. For comparison, other parameter values were the same in all the calculations. Figures 1(b) and 1(c) show the calculated performances of the SCSCs before and after the SF method was applied. Before the SF method was applied [Fig. 1(b)], P was highest at $\lambda = 0$, where power dissipation is not considered in the design. P decreased with λ, while RMS ΔB_0 increased. This result ensures the validity of the power optimization algorithm. After the SF method was applied [$\sigma = 58.2$ mm, Fig. 1(c)], RMS ΔB_0 increased and P decreased for all values of λ, as described earlier. P was highest (7.17 W) at $\lambda = 0$, and decreased with λ, while RMS ΔB_0 increased. When $\lambda > 0.05$, RMS ΔB_0 and P were almost constant. In contrast, RMS ΔB_0 was not a minimum at $\lambda = 0$ but slightly larger than that for $\lambda = 0.005$ [Fig. 1(c)], because the errors due to the Gaussian filtering in the SF method varied with λ. We determined the optimized value of λ to be 0.005, because P was then only 1.79 W, which was 75% smaller than that for the nonoptimized coil ($\lambda = 0$), while RMS ΔB_0 decreased to the same level as the nonoptimized coil.

To demonstrate the validity of the power optimization, two coil patterns were fabricated, namely, a nonpower-optimized coil (SC1, $\lambda = 0$) and a power-optimized coil (SC2, $\lambda = 0.005$). Each coil was fabricated by winding a polyethylene-coated Cu wire (0.6 mm in diameter) fixed on a fiber-reinforced plastic plate ($36 \times 36\,\text{cm}^2$, 0.5 mm thick) using epoxy resin [Fig. 2(a)]. Each SCSC was inserted between the gradient coil and the pole piece [Fig. 2(b)], and the B_0 map with shimming was measured. The field inhomogeneity $\Delta B_0(\mathbf{r})$ was calculated from the measured map as $\Delta B_0(\mathbf{r}) = B_0(\mathbf{r}) - B_0(\mathbf{0})$.

Table I. RMS and peak-to-peak (PP) ΔB_0 (ppm) over a $12 \times 16 \times 5\,\text{cm}^3$ DEV, for current I (A), resistance R (Ω), and power dissipation P (W).

		λ	RMS ΔB_0	PP ΔB_0	I	R	P
Initial		—	24.8	235	—	—	—
Calc.	SC1	0	15.6	189	1.79	2.24	7.17
	SC2	0.005	14.9	182	1.02	1.72	1.79
Meas.	SC1	0	14.0	195	1.20	2.74	3.95
	SC2	0.005	14.2	196	0.70	2.14	1.05

Table I summarizes the calculated and measured performances for SC1 and SC2. For each coil, the shim current I was optimized to minimize RMS ΔB_0.[4,5,7] For both coils, the measured values of RMS and peak-to-peak ΔB_0 were almost the same as the calculated values, indicating the accuracy of the design and fabrication of the coil. However, the measured values of I and P were smaller than the calculated values for both SC1 and SC2. This is possibly

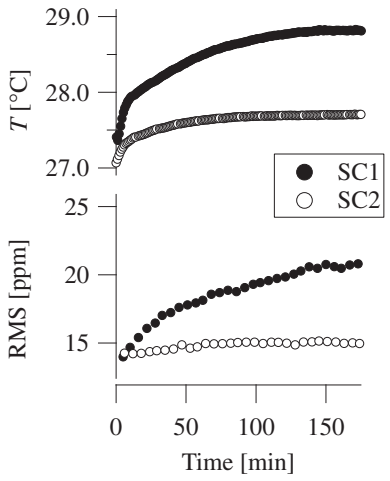

Fig. 3. Temperature change of the pole-piece surface and RMS ΔB_0, after the SCSC was switched on.

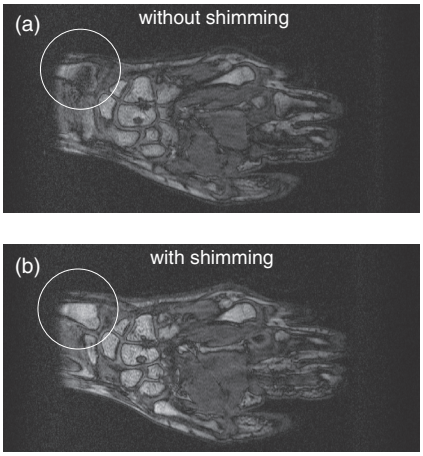

Fig. 5. Gradient echo images of a left hand (a) without and (b) with shimming by SC2.

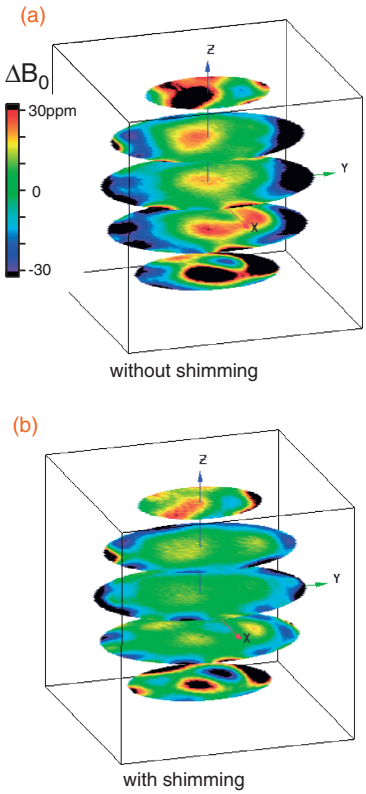

Fig. 4. ΔB_0 maps (in a $12 \times 16 \times 5\,\mathrm{cm}^3$ DEV) measured (a) without and (b) with shimming by SC2.

because the mirror current flowing in the pole piece enhances the magnetic field generated by the SCSC[10] and a smaller current would have been sufficient for shimming.

Figure 3 shows the evaluation of the heat generated by SC1 and SC2 after the SCSC was switched on. For the nonoptimized SC1, the temperature T of the pole-piece surface had increased by about 1.4 °C, and the RMS ΔB_0 had increased by 6.8 ppm after 170 min, and both kept increasing thereafter. This indicates that the high heat degraded the B_0 homogeneity to an unacceptable level. In contrast, for the power-optimized SC2, T and RMS ΔB_0 increased by only 0.6 °C and 0.8 ppm, respectively, after 100 min, and remained almost constant thereafter. This shows that the power-optimized SC2 can effectively suppress both heat generation and B_0 degradation.

Figures 4 and 5 illustrate the performance of the fabricated SC2. Figure 4 shows three-dimensional ΔB_0 maps measured (a) without and (b) with shimming by SC2. This demonstrates that the B_0 inhomogeneity was largely corrected by shimming over the whole area. Figure 5 shows two-dimensional cross-sectional images (taken from three-dimensional images of the left hand of a volunteer) obtained (a) without and (b) with shimming using a gradient echo sequence (FOV $= 10 \times 20 \times 5\,\mathrm{cm}^3$, matrix $= 128 \times 512 \times 32$, TR $= 40$ ms, TE $= 11$ ms, and flip angle $= 60°$). A part of the ulna bone (circled in the images) was invisible without shimming, a signal-loss artifact due to B_0 inhomogeneity. In contrast, this image artifact was removed by shimming. The improvement in the image quality enables accurate visualization of the anatomical structure of bones, which is necessary for applications such as skeletal age assessment in children using MRI.[11]

In summary, we have proposed a power optimization method for designing a planar SCSC for a permanent MRI magnet. The power-optimized SCSC achieved a B_0 homogeneity comparable to that of a nonpower-optimized SCSC, but with negligible heat generation.

1) W. A. Anderson: Rev. Sci. Instrum. **32** (1961) 241.
2) F. Roméo and D. I. Hoult: Magn. Resonance Med. **1** (1984) 44.
3) R. Shigeki and K. Kose: Proc. Int. Soc. Magn. Reson. Med. **19** (2010) 1542.
4) D. Tamada, Y. Terada, and K. Kose: Appl. Phys. Express **4** (2011) 066702.
5) D. Tamada, K. Kose, and T. Haishi: Appl. Phys. Express **5** (2012) 056701.
6) Y. Terada, S. Kono, K. Ishizawa, S. Inamura, T. Uchiumi, D. Tamada, and K. Kose: submitted to J. Magn. Resonance.
7) Y. Terada, D. Tamada, and K. Kose: J. Magn. Resonance **212** (2011) 355.
8) C. Juchem, T. W. Nixon, S. McIntyre, D. L. Rothman, and R. A. de Graaf: J. Magn. Resonance **204** (2010) 281.
9) C. Juchem, T. W. Nixon, S. McIntyre, V. O. Boer, D. L. Rothman, and R. A. de Graaf: J. Magn. Resonance **212** (2011) 280.
10) S. Handa, K. Kose, and T. Haishi: Proc. Intl. Soc. Magn. Reson. Med. **17** (2009) 3069.
11) Y. Terada, S. Kono, D. Tamada, T. Uchiumi, K. Kose, R. Miyagi, E. Yamabe, and H. Yoshioka: Magn. Resonance Med. (in press) [DOI: 10.1002/mrm.24439].